CHAPTER 6

CHAPTER 6

Geochemistry

Geochemical analysis was carried out to understand the protolith history, metamorphic changes and probable tectonic setting for a rock suite. Major, trace and rare earth element (REE) geochemical characters of the high-grade rocks of the Central Gneissic Belt are expected to highlight the evolution of the deeper crustal section of the Rengali Province.

6.1 Analytical methods

Major and trace elements were analyzed using XRF while REE analyses were carried out using LA-ICPMS at the Hiroshima University, Japan. For whole rock chemical analysis, representative samples were cleaned with deionized water and crushed using Jaw Crusher to smaller chip size. The chips were later made powders using the Retsch Pulverizer at the Presidency University. The powdered samples were dried in an oven at 120°C for 12 hours and then for 6 hours at 950°C to estimate the LOI. Subsequently, these samples were fused into glass discs using an oven-dried alkali flux, Johnson Matthey Spectroflux 100B [a mixture of lithium tetraborate (Li2B4O7) and lithium metaborate (LiBO2) with a mixing ratio of 2:8] and lithium nitrate (LiNO3) as an oxidizing agent. The discs were prepared from 2.0 gm. of rock powder, 4.0 gm. of flux and 0.60 gm. of LiNO3 as an oxidizer and ~100 µL of 5% LiI solution added to prevent adhesion to the Pt crucible. Whole-rock geochemical analyses for major and trace elements of the samples were carried out by X-ray fluorescence techniques using a Rigaku ZXS system equipped at Hiroshima University, Japan. X-rays generated by a 3kW Rh-W dual anode tube were radiated on fused bead samples. Rare earth elements were measured by LA-ICP-MS (Agilent 7500 series coupled with 213 nm Nd-YAG

Laser of New Wave ResearchUP-213) on fused sample glass at Hiroshima University, Japan. NIST 610 and NIST 612 standards were used for calibration.

6.2 Major element geochemistry

6.2.1 Charnockite gneiss

Representative samples of charnockite gneiss have been analyzed for major, trace and REE geochemistry (Table 6.1). In charnockite gneiss, SiO_2 contents vary within a small range (66.73-71.27 wt.%). These rocks have low TiO_2 contents (0.38 to 0.86 wt.%), moderate Al_2O_3 (11.60–12.90 wt.%), FeOt (3.95–5.81 wt.%), MgO (0.16–0.78 wt.%) and CaO (1.19-2.68 wt.%). Total alkali contents are high and in the range of 7.53–8.17 wt.% while Mg# shows a restricted range of 6.77 to 20.15. Except one sample, other five analyses of charnockite gneiss plot within the field of granite in the total alkali vs. silica diagram (Fig. 6.1; Cox et al., 1979). The other sample plots at the boundary between granite and quartz diorite fields. When plotted in the granite classification diagram of Frost et al. (2001), the charnockite gneiss samples show a ferroan affinity with a Fe-number [SiO_2 vs. Fe*/(Fe*+Mg)O; where Fe*= FeO_{total}] varying between 0.88-0.96 (Fig. 6.2a). In terms of modified alkali-lime index (MALI), the charnockite samples show value in the range between 5.03 and 6.72 and are alkali-calcic to calc-alkalic in nature (Fig. 6.2b) and with respect to alumina saturation index (ASI) are metaluminous in character with a value between 0.87 and 0.98 (Fig. 6.2c).

6.2.2 Migmatitic hornblende gneiss

Representative samples of migmatitic hornblende gneiss of the Central Gneissic Belt were analyzed (Table 6.1). The major element chemistry of the migmatitic hornblende gneisses is marked by high SiO_2 (71.53–73.19 wt.%), low TiO_2(0.34–0.57 wt.%), moderate

Al_2O_3(12.36–13.33 wt.%), FeOt (2.13–3.91 wt.%), MgO (0.23–0.57 wt.%) and CaO (1.07–1.90 wt.%). Total alkali contents are high within a range of 8.25–8.42 wt.%. Mg# shows a restricted range of 12.04-21.14. All the migmatitic hornblende gneiss samples fall within the field of granite in the total alkali vs. silica diagram (Fig. 6.1; Cox et al., 1979). In case of these samples, when plotted in the granite classification diagram of Frost et al. (2001), show a ferroan affinity with a Fe-number [SiO_2 vs. Fe*/(Fe*+Mg)O; where Fe*= FeO_{total}] varying between 0.86-0.93 (Fig. 6.2a). In terms of MALI, the charnockite gneiss samples show values in the range of 6.36 and 7.35 (Fig. 6.2b) and are alkali-calcic to calc-alkaline in nature. Samples show both metaluminous and weakly peraluminous character with a value between 0.93 and 1.00 (Fig. 6.2c).

6.2.3 Felsic gneiss

The major element chemistry of the felsic gneiss is marked by high SiO_2 (72.6-74.7 wt.%), low TiO_2(0.11–0.36wt.%), MgO (0.04–0.32 wt.%), moderate Al_2O_3(11.82–13.96 wt.%), FeOt (1.66–3.89 wt.%), and CaO (1.10–1.28 wt.%) (Table 6.1). Total alkali contents are high within a range of 8.25–8.42 wt.%. Mg# varies widely in the range of 3.82-16.71. All the felsic gneiss samples plot within the field of granite in the total alkali vs. silica diagram (Fig. 6.1; Cox et al., 1979). In case of these samples, when plotted in the granite classification diagram of Frost et al. (2001), show a ferroan affinity with a Fe-number [SiO_2 vs. Fe*/(Fe*+Mg)O; where Fe*= FeO_{total}] varying between 0.89-0.98 (Fig. 6.2a). In terms of MALI, the samples show value in the range between 6.57 and 7.51 and are calc-alkalic in nature (Fig. 6.2b). Samples show both metaluminous and peraluminous character with a value between 0.97 and 1.13 (Fig. 6.2c).

6.2.4 Mafic granulite

Mafic granulite which occurs as enclaves within charnockite gneiss is marked by intermediate SiO_2 (49–56 wt.%), high TiO_2 (1.24-1.51 wt.%), Al_2O_3(~13.5 wt.%), high FeOt (~12 wt.%), MgO (3.2-6.6 wt.%) and CaO (8.15-11.5 wt.%) (Table 6.1). Mafic granulite samples plot within the field of gabbro and diorite in the total alkali vs. silica diagram (Fig. 6.1; Cox et al., 1979).

6.2.5 Amphibolite

Amphibolite is present as enclaves within the basement felsic gneiss within the central part of Rengali Province. SiO_2 content of these rocks vary between 50-54%, while TiO_2 content varies in the range 0.95-1.07 wt.%. These along with FeOt (11.64-13.96 wt.%) and CaO (9.62-10.66 wt.%) contents of the samples plot within the field of gabbro in the total alkali vs. silica diagram (Fig. 6.1; Cox et al., 1979). Mg# shows a value within a narrow range of 42.03-45.91(Table 6.1).

6.3 Trace and REE geochemistry

Though major element concentrations were measured for the high-grade rocks of Central Gneissic Belt, much reliance was given on trace element and REE geochemistry. This is because the major elements are usually mobilized easily during high-temperature conditions, thereby proved ambiguous in preserving the original pre-metamorphic characters. On the contrary, the REEs are much robust in preserving the protolith history of high-grade rocks.

6.3.1 Charnockite Gneiss

Charnockite gneiss shows moderate range of variation in transitional trace element compositions (Ni: 5.9-14.4 ppm; Cr: 6.1-20.9 ppm; Co: 91.5-154.6 ppm); high concentration

of Zr (668.2-998.7 ppm) and Ba (964.8-1171.2 ppm) (Table 6.1). When the trace elements were plotted in the tectonic discrimination diagram of Whalen et al. (1987), an A-type granite character is indicated (Fig. 6.3). Tectonic discrimination diagram of Pearce et al. (1984) for trace involving elements like Nb, Ta, Y, Yb also suggest within-plate (WPG) tectonic setting (Fig. 6.4). Compositions of most of the samples plot within the field of A2 subgroup of A-type granites in the ternary discrimination diagram (Fig. 6.5) after Eby (1992), which implies a variety of tectonic settings including the post-collisional setting. Chondrite-normalized REE patterns (Fig. 6.7) for the charnockite gneiss samples show a LREE enrichment [(La/Sm)N = 3.32-5.23] and a flat HREE pattern [(Gd/Yb)N ratio = 1.20] with a pronounced negative Eu anomaly [(Eu/Eu*)= 0.54-0.64]. Total REE content ranges between 469.82- 563.61.

6.3.2 Migmatitic hornblende gneiss

Migmatitic hornblende gneiss shows a moderate range of variation in transitional trace element compositions (Ni: 5.07-9.8 ppm; Cr: 6.7–11.9 ppm, Co: 109.9–187.6 ppm),; high concentration of Zr (353.1-778.8 ppm) and Ba (886.94-1074.1 ppm) (Table 6.1). When the trace elements are plotted in the tectonic discrimination diagram of Whalen et al. (1987), again an A-type granite character is indicated (Fig. 6.3). Tectonic discrimination diagram of Pearce et al. (1984) for trace involving elements like Nb, Ta, Y, Yb also suggest within-plate (WPG) tectonic setting (Fig. 6.4). Chondrite-normalized REE patterns (Fig. 6.7) for these migmatitic hornblende gneiss samples show a LREE enrichment [$(La/Sm)_N$ =5.22-9.70] and a flat HREE pattern $(Gd/Yb)_N$ ratio = 1.18-1.94Yb) with a pronounced negative Eu anomaly [(Eu/Eu*)=0.44-0.99]. Total REE content ranges between 469.82- 563.61. Overall REE content for migmatitic hornblende gneiss samples display a greater variation (∑REE contents = 389.24- 672.78).

6.3.3 Felsic gneiss

Felsic gneiss shows moderate range of variation in transitional trace element compositions (Ni: 3.88-6.74; Cr: 3.81-5.21; Co: 118.5-136.2); moderate concentration of Zr (223.72-790.67 ppm) and Ba (385.04-950.86 ppm) (Table 6.1). When the trace elements are plotted in the tectonic discrimination diagram of Whalen et al. (1987), A-type granite character is indicated (Fig. 6.3). Tectonic discrimination diagram of Pearce et al. (1984) for trace involving elements like Nb, Ta, Y, Yb also suggest within-plate (WPG) tectonic setting (Fig. 6.4). Chondrite-normalized REE patterns (Fig. 6.7) for these felsic gneiss samples show a LREE enrichment [$(La/Sm)_N$ = 4.87-6.10] and a flat HREE pattern (Gd/Yb)N ratio = 1.29-1.72 with a pronounced negative Eu anomaly [(Eu/Eu*)=0.26-0.61]. Total REE content ranges between 469.82- 563.61. Overall REE content for migmatitic hornblende gneiss samples display a greater variation (∑REE contents = 335- 767.86).

6.3.4 Mafic rocks (mafic granulite, amphibolite and metadolerite)

Transitional element concentration in mafic granulite, amphibolite and metadolerite is low to medium (Cr- 10.76- 149 ppm; Ni- 47.47-108.66), whereas in one sample concentration is extremely high (Cr- 1710 ppm; Ni- 429.2 ppm). Concentration of Ba is low (84.56- 339.72 ppm) (Table 6.1). Tectonic discrimination diagram (Pearce and Norry, 1979; Meschede, 1996) involving trace elements (Y, Zr, Nb) for the mafic granulite, metadolerite and amphibolite samples suggest a within-plate tectonic setting (Fig. 6.6).

The overall REE pattern suggests a similar source of all the granitoids and charnockite rocks. Tectonic discrimination diagrams for both acidic and basic rocks helped to identify their tectonic environment which implies a within-plate tectonic setting for the rocks.

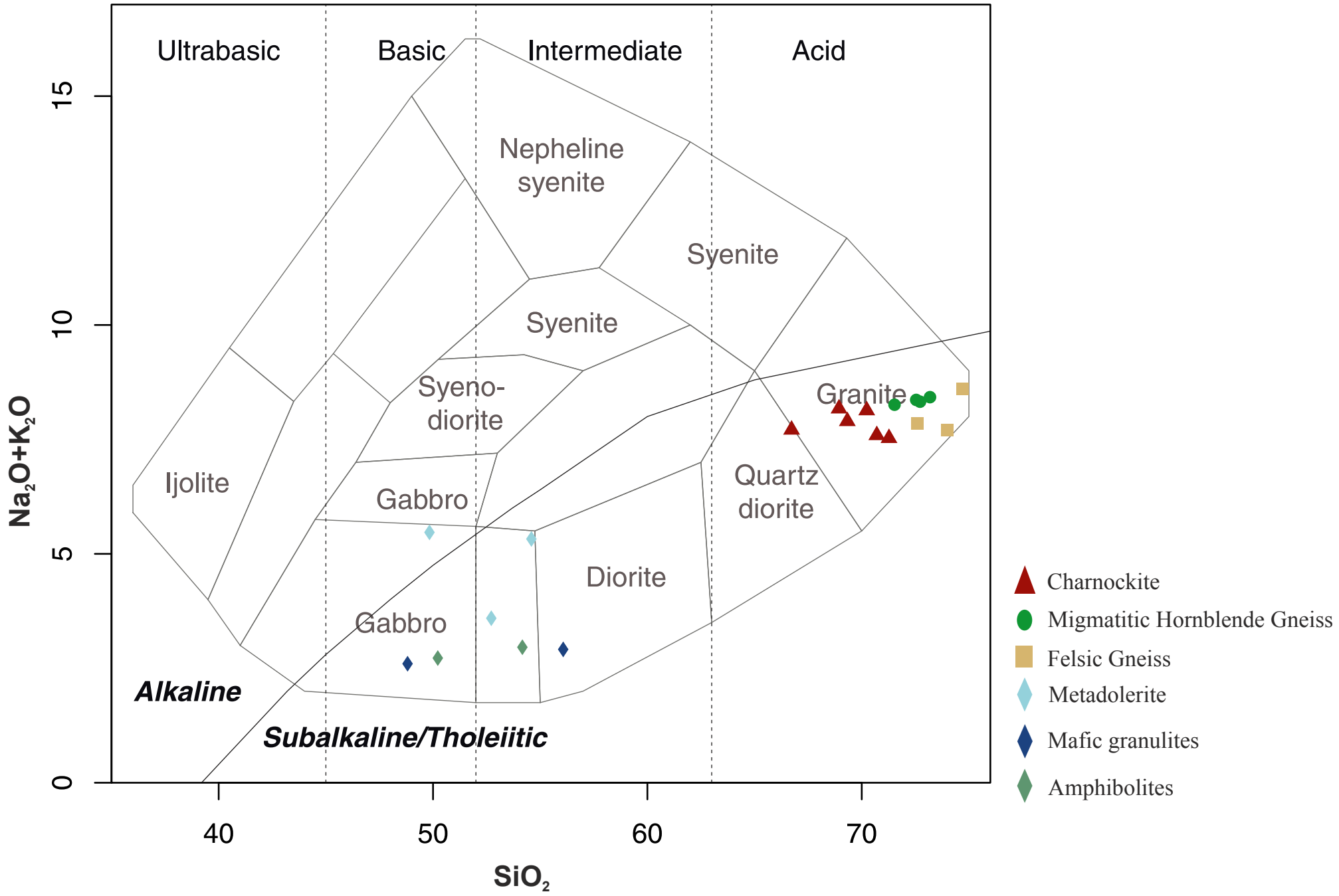

Fig. 6.1: Total alkali vs. silica (TAS) classification diagram of all the high-grade rocks of the Central Gneissic Belt (after Cox et al., 1979).

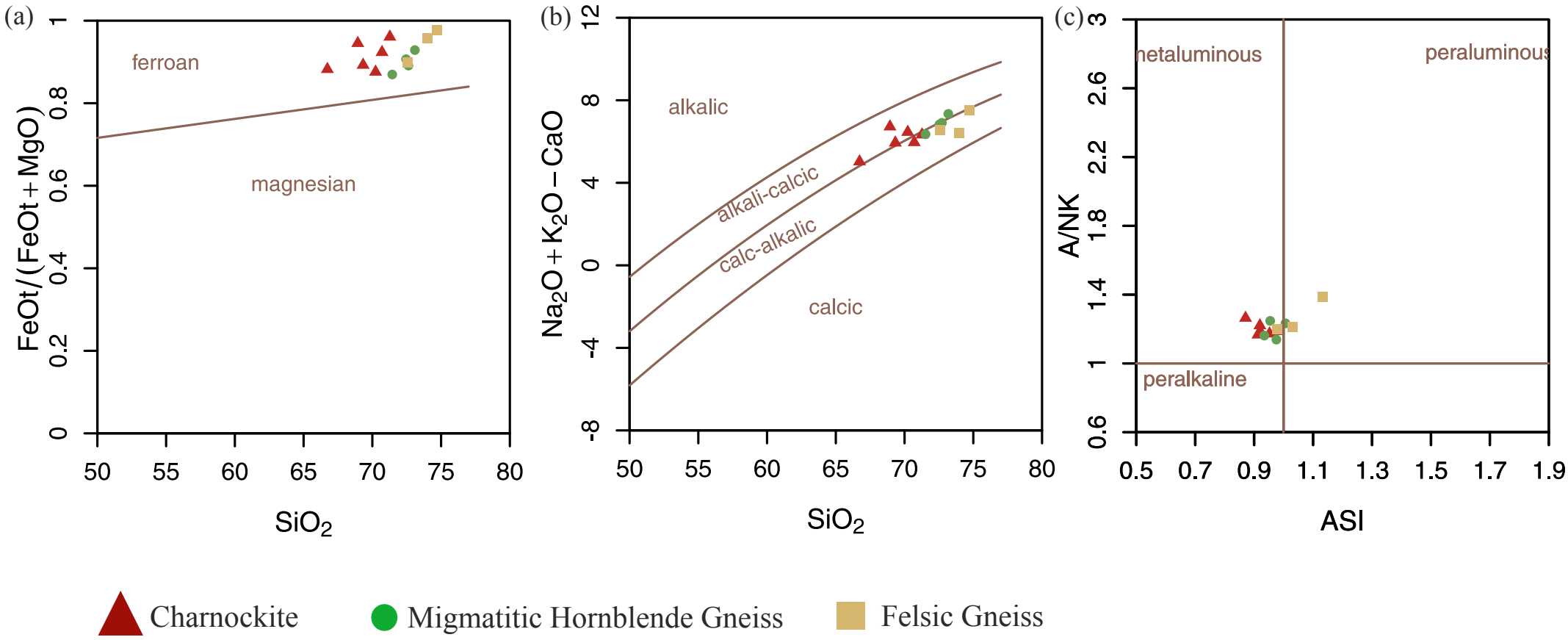

Fig. 6.2: (a)Fe-number [*Fe*/(Fe*+MgO) vs. SiO_2*] plot. (b) Modified Alkali-lime index (Na_2O+K_2O-CaO vs. SiO_2) plots. (c)Alumina saturation index plot illustrating the grouping of charnockite and other granitoid gneisses from Central Gneissic Belt, after the classification of Frost et al. (2001).

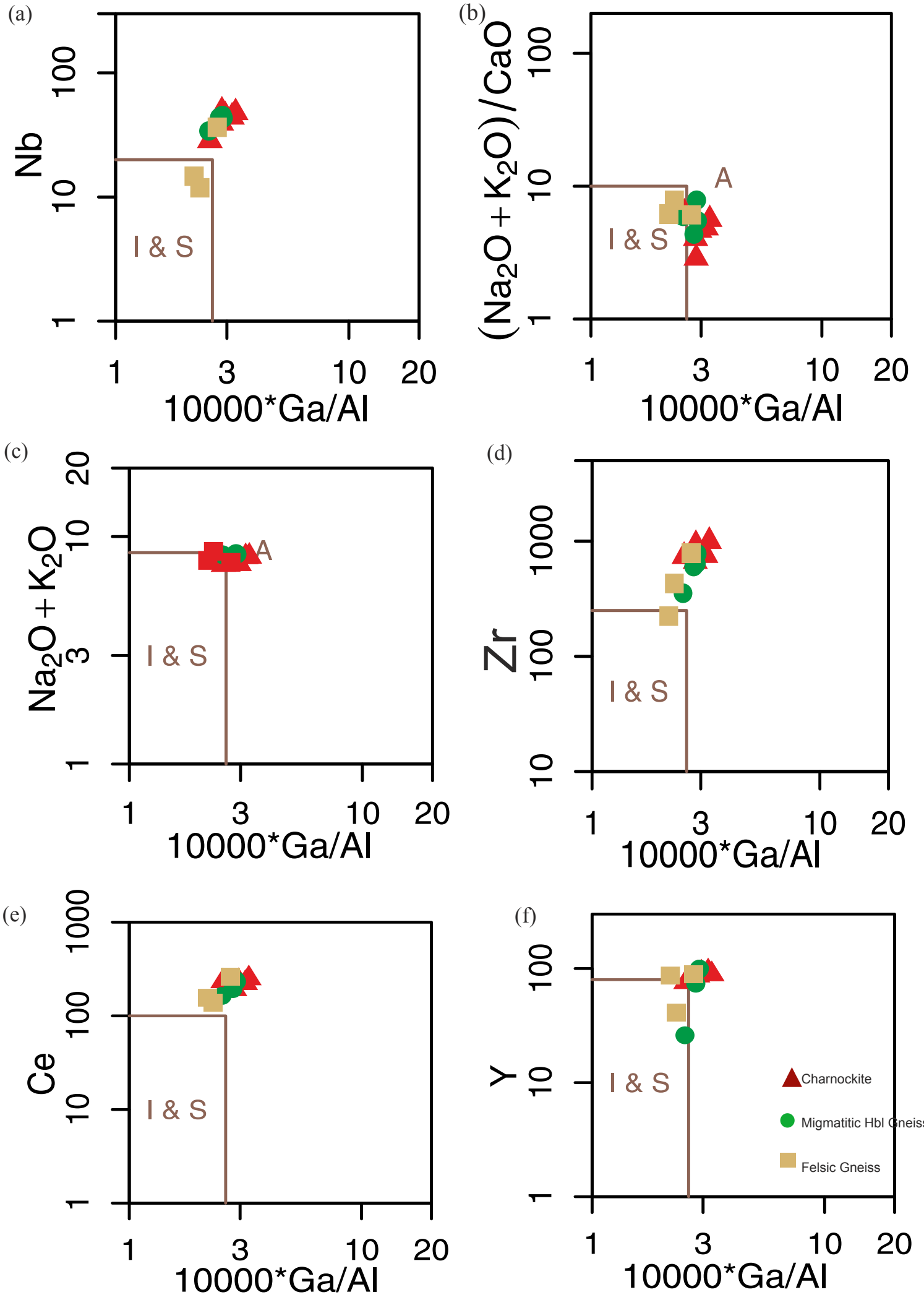

Fig. 6.3: Multi element vs Ga/Al bivariate plot, after Whalen (1987) of granitoids and charnockite from Central Gneissic Belt.

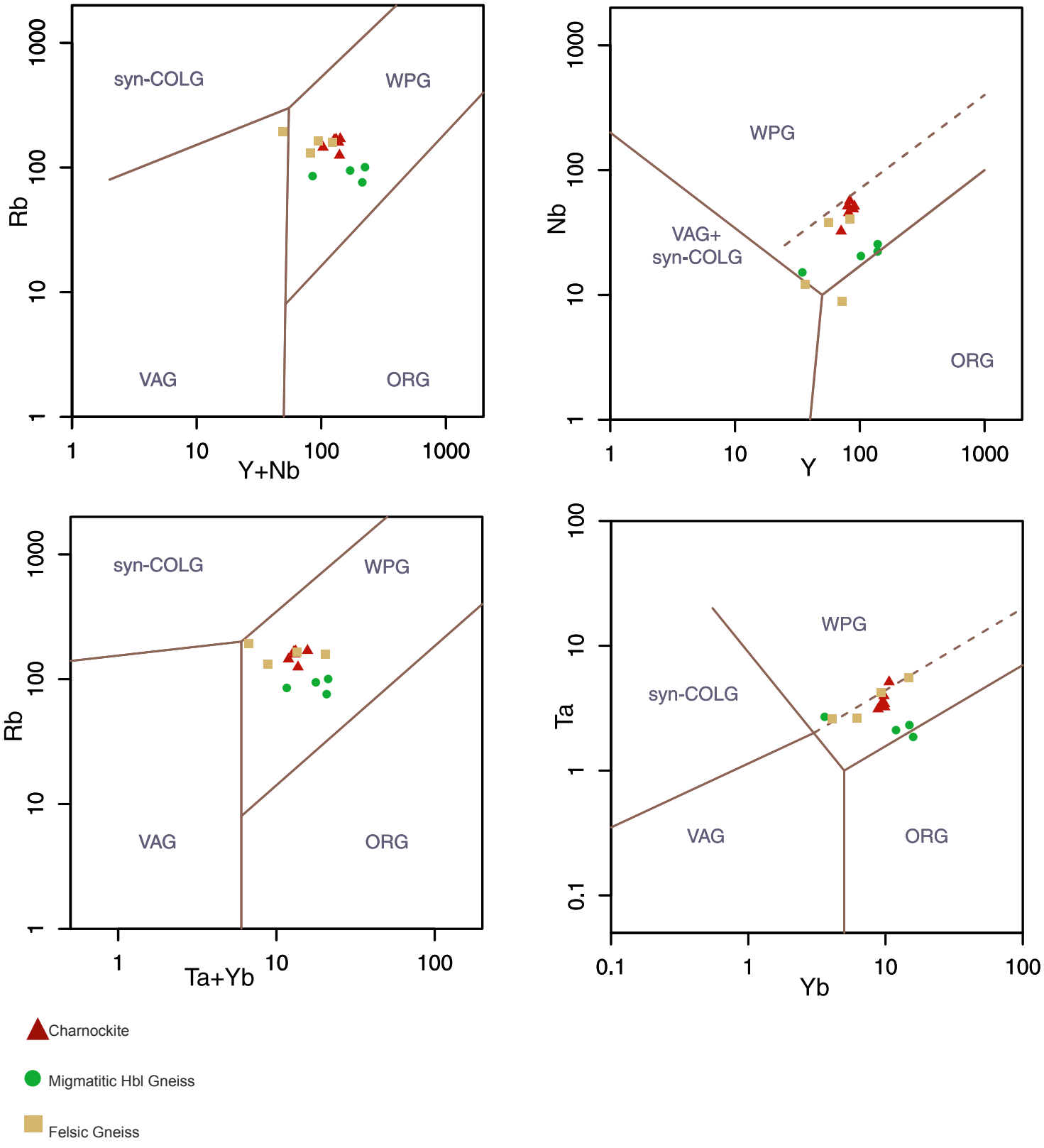

Fig. 6.4: Plot of trace and REE elements of the granitoids and charnockite from the Central Gneissic Belt, according to the tectonic discrimination diagram of Pearce (1984).

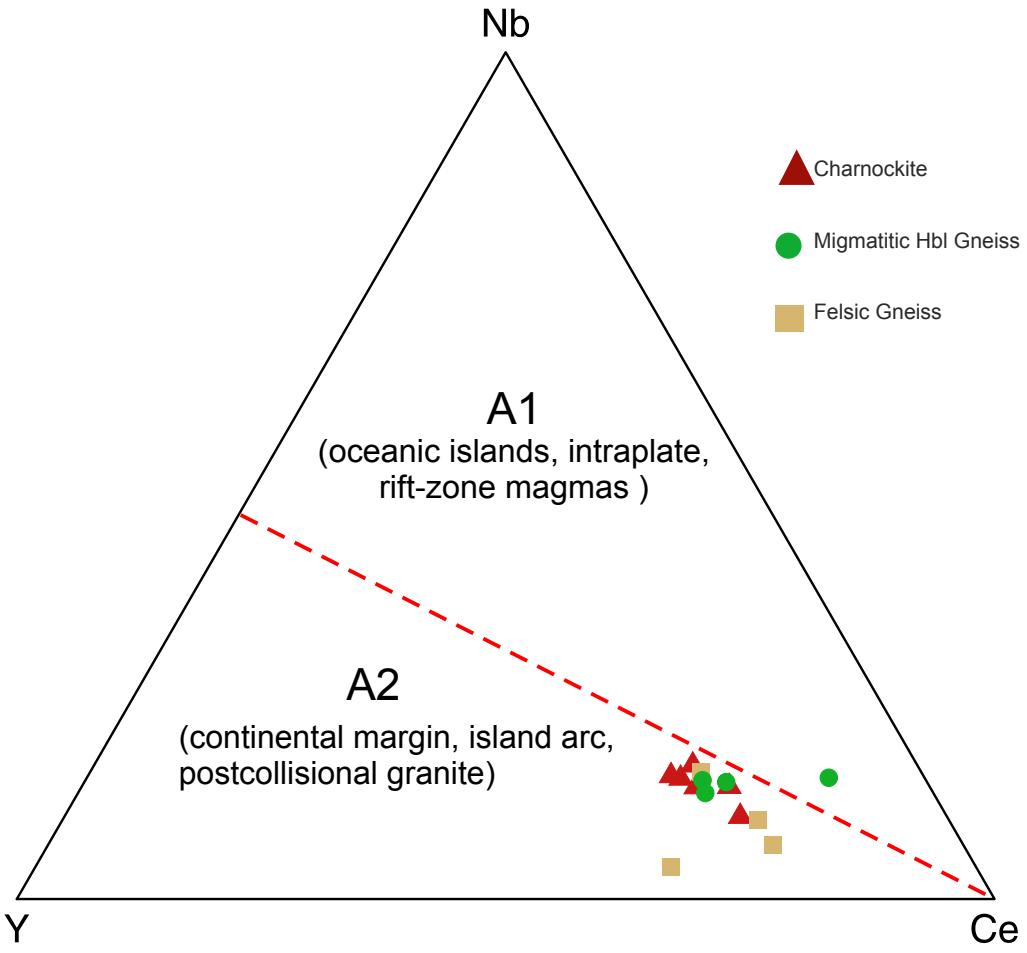

Fig. 6.5: Triangular plot of Eby (1992), used to distinguish between A1 and A2 type granite. Here, most of the granitoids and gneisses from Central Gneissic Belt plot in the field of A2 granite, which suggests a origin involving collision or subductional setting.

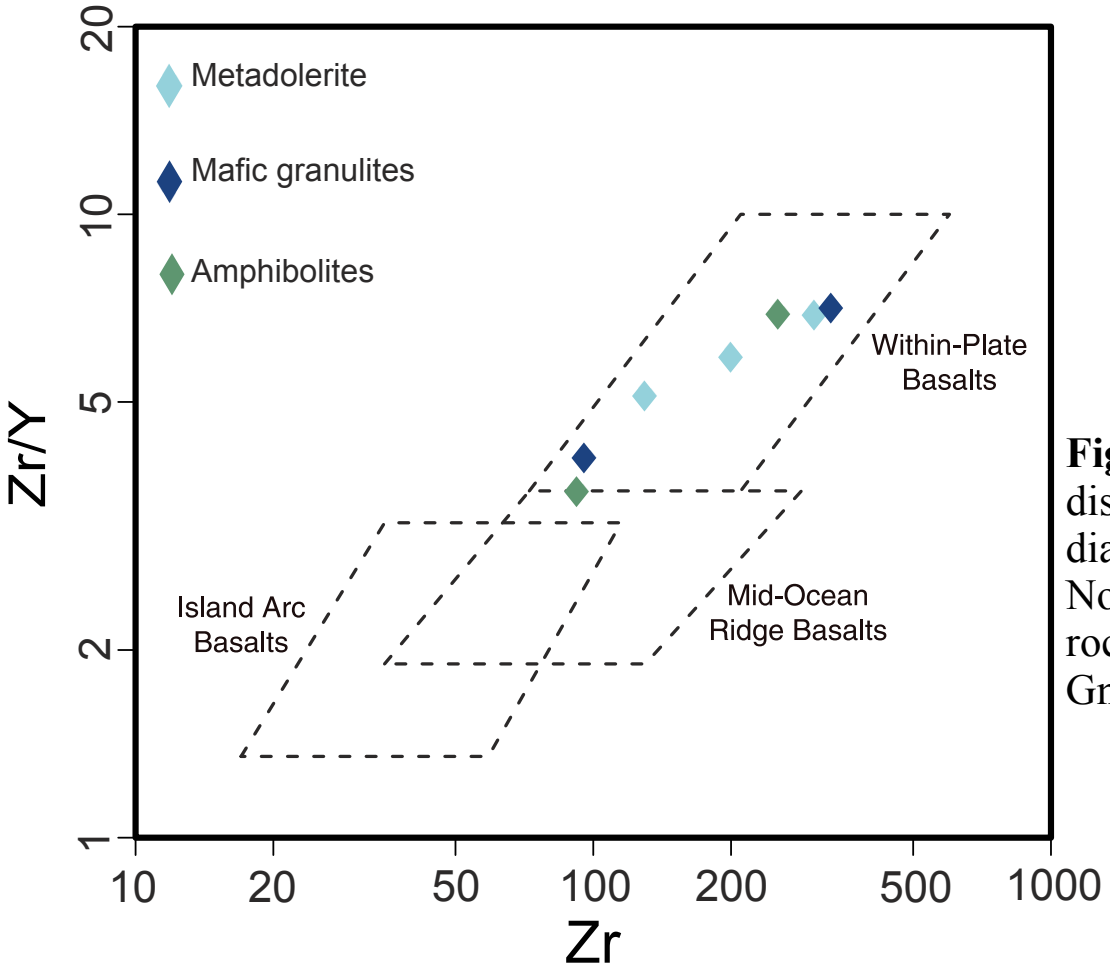

Fig. 6.6: Tectonic discrimination diagram (Pearce and Norry, 1979) of mafic rocks from Central Gneissic Belt.

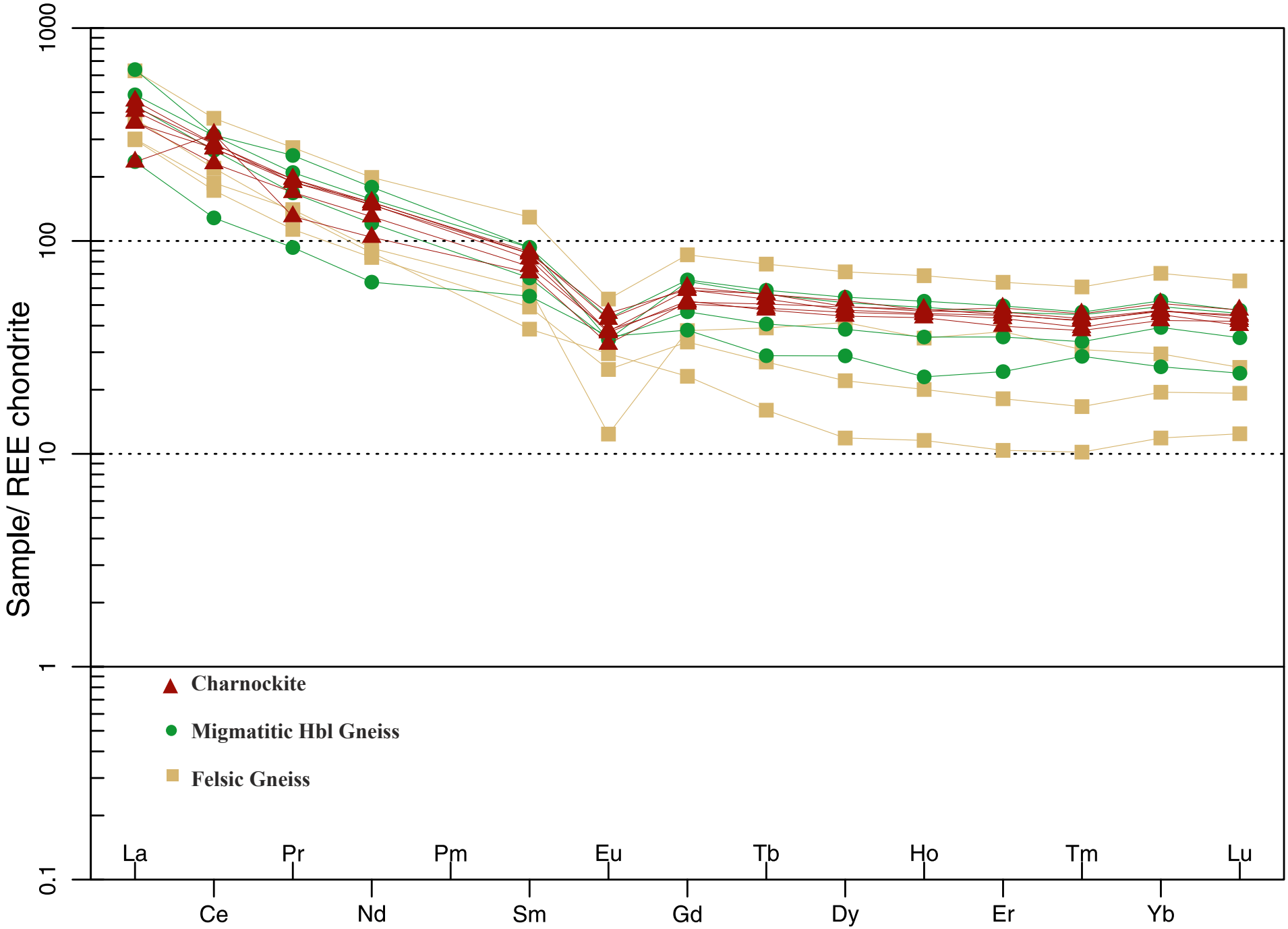

Fig. 6.7: Chondrite-normalized REE spider plot of charnockite, migmatitic hornblende gneiss and felsic gneiss of Central Gneissic Belt.

Table 6.1: Major, trace and REE analytical data from representative samples of the Central Gneissic Belt

Rocks	*Felsic gneiss*				*Migmatitic hornblende gneiss*				*Charnockite*						*Amphibolite*		*Mafic granulite*		*Metadolerite*		
Sample no.	**JK60B**	**RNG51B**	**RNG175**	**RNG54D**	**RNG145C**	**RNG123A**	**RNG131**	**RNG146C**	**RNG158**	**RNG120A**	**RNG129A**	**RNG165**	**RNG53E**	**RNG133**	**RNG144A**	**RNG138A**	**RNG 122**	**RNG 157B**	**RNG 145B**	**RNG 52B**	**RNG 53A**
(wt.%)																					
SiO_2	72.10	72.59	74.00	74.70	71.53	72.54	73.19	72.72	70.70	66.73	70.23	71.27	69.33	68.94	54.15	50.21	56.01	48.724	54.54	49.78	52.67
TiO_2	0.56	0.11	0.36	0.14	0.57	0.49	0.42	0.34	0.50	0.85	0.55	0.38	0.61	0.56	0.95	1.07	1.244	1.515	0.90	2.20	0.48
Al_2O_3	13.17	13.96	11.82	13.60	13.21	12.54	12.36	13.33	11.60	12.90	12.16	11.60	12.54	12.42	14.23	15.53	13.35	13.94	13.22	13.50	8.43
Fe_2O_3	4.15	3.14	4.32	1.84	4.23	4.35	3.39	2.36	4.94	6.46	4.65	4.39	4.42	5.41	12.93	15.51	13.33	13.78	11.49	15.74	10.77
MnO	0.07	0.05	0.07	0.05	0.05	0.06	0.06	0.04	0.08	0.08	0.07	0.06	0.06	0.08	0.18	0.25	0.18	0.21	0.15	0.19	0.17
MgO	0.55	0.32	0.17	0.04	0.57	0.40	0.23	0.26	0.37	0.78	0.59	0.16	0.48	0.28	5.54	5.68	3.24	6.61	4.01	4.11	14.90
CaO	1.52	1.28	1.27	1.10	1.90	1.52	1.07	1.41	1.63	2.68	1.68	1.19	1.96	1.45	9.62	10.66	8.15	11.495	8.12	7.89	7.02
Na_2O	3.57	2.79	2.71	3.38	2.88	3.04	3.03	3.15	2.80	3.30	2.88	2.88	3.07	3.09	2.34	2.19	2.59	2.33	3.92	4.06	2.40
K_2O	5.09	5.06	4.99	5.23	5.38	5.33	5.39	5.18	4.79	4.41	5.26	4.65	4.83	5.09	0.60	0.52	0.32	0.26	1.42	1.43	1.21
P_2O_5	0.07	0.07	0.06	0.03	0.14	0.09	0.08	0.07	0.13	0.21	0.11	0.07	0.15	0.15	0.17	0.15	0.24	0.14	0.14	0.41	0.06
LOI	0.45	0.00	0.13	0.15	0.16	0.16	0.25	0.30	0.71	0.35	0.58	0.50	0.32	0.31	0.97	0.35	0.73	0.63	0.17	0.01	0.01
Total	101.30	99.36	99.89	100.25	100.61	100.53	99.48	99.16	98.25	98.76	98.77	97.15	97.77	97.78	101.69	102.10	99.37	99.63	98.07	99.31	98.10

b.d. Below detection limit

Table 6.1 contd.

Rocks	*Felsic gneiss*				*Migmatitic hornblende gneiss*				*Charnockite*						*Amphibolite*		*Mafic granulite*		*Metadolerite*		
Sample no.	**JK60B**	**RNG51B**	**RNG175**	**RNG54D**	**RNG145C**	**RNG123A**	**RNG131**	**RNG146C**	**RNG158**	**RNG120A**	**RNG129A**	**RNG165**	**RNG53E**	**RNG133**	**RNG144A**	**RNG138A**	**RNG 122**	**RNG 157B**	**RNG 145B**	**RNG 52B**	**RNG 53A**
(in ppm)																					
Sc	6.35	5.63	4.18	4.37	6.36	5.71	4.14	1.88	5.76	11.35	5.84	3.43	7.04	7.89	35.28	43.13	32.73	41.71	28.74	28.59	28.24
V	33.45	5.62	7.92	4.55	31.46	17.4	11.89	14.28	21.01	38.28	21.52	9.03	25.98	20.28	229.83	333.41	258.43	303.81	220.59	297.77	157.88
Cr	15.02	5.21	4.89	3.81	10.44	11.94	6.67	8.54	7.24	10.14	20.89	6.94	8.04	6.16	12.98	126.71	10.76	149.04	39.82	54.65	1710.72
Co	93.16	118.52	136.21	130.84	109.88	131.07	152.09	187.61	109.71	127.78	154.58	142.67	91.47	99.71	91.89	87.99	108.56	101.2	94.59	68.75	91.57
Ni	9.31	6.74	3.88	4.05	8.09	9.78	5.48	5.07	6.3	8.63	14.41	8.19	5.93	8.42	78.41	108.66	47.47	56.8	46.04	74.10	429.26
Cu	14.38	7.54	17.24	7.47	9.96	15.04	7.64	11.59	18.19	26.72	11.03	13.64	17.91	13.17	34.21	47.32	74.92	50.13	78.05	43.60	58.70
Zn	125.24	18.58	106.25	56.74	73.04	93.54	87.96	63.44	109.97	128.07	102.96	111.38	85.13	128.56	102.54	111.18	88.56	102.44	109.31	144.91	81.56
Ga	19.11	16.03	17.05	16.53	19.51	19.2	18.76	17.69	18.13	19.49	20.31	15.56	18.84	21.49	18.07	20.3	17.79	18.58	16.95	21.45	10.07
Rb	193.71	131.21	163.75	158.75	208.24	167.45	221.41	187.87	159.02	125.13	169.69	144.98	166.42	167.97	9.51	13.64	2.42	6.8	73.13	29.45	74.39
Pb	39.55	45.65	31.93	26.19	37.83	33.35	38.66	46.9	31.31	26.9	32.65	28.4	29.37	36.34	4.2	5.3	6.4	0.79	11.40	13.95	7.41
Cs	9.24	4.35	8.32	1.05	7.4	9.8	6.24	6.18	10.77	10.71	7.7	9.38	8.36	8.78	b.d	0.5	1.72	b.d	2.51	0.18	2.20
Ba	837.64	385.04	950.86	593.54	1003.78	1074.14	886.94	893.51	964.82	1171.16	1108.85	1033	1003.13	1035.91	138.11	156.56	84.56	98.02	242.92	339.72	127.55
Sr	109.2	103.7	54.6	32.8	83.2	63.3	42.5	81.9	63.68	93.29	61.97	80.46	75.47	54.72	168.1	158	190.59	214.34	145.48	168.49	66.00
Y	56.5	72.6	83.6	36.7	67.4	91.8	91.9	22.9	88.63	82.90	90.29	70.68	81.14	79.76	25.6	36.6	46.66	23.57	33.67	43.76	25.27
Zr	515	232.2	798.8	455.4	627.4	779	689	363	813.30	970.09	843.83	815.37	716.93	1092.23	91.9	253	330.25	95.77	199.75	303.96	129.56
Nb	37.91	8.84	40.25	12.15	45.31	49.27	56.42	33.5	48.92	57.04	51.49	32.53	45.69	51.64	3.51	15.06	20.32	6.03	13.44	19.17	9.78
La	113.55	93.42	195.19	92.62	133.85	150.55	197.8	115.87	141.19	110.97	126.13	132.20	112.20	72.93	28.82	73.14	50.53	22.29	43.35	54.10	31.05
Ce	157.09	151.44	304.58	139.54	215.36	252.46	253.85	177.46	231.60	220.26	218.80	230.27	186.73	256.87	24.38	103.69	90.53	19.64	63.27	86.03	39.41
Pr	19.24	17.12	33.49	13.82	20.51	25.56	30.76	16.59	23.04	23.04	23.86	23.79	20.64	15.89	3.01	11.36	10.87	2.95	7.78	9.67	4.22
Nd	71.93	55.49	119.29	50.19	72.56	94.14	107.34	52.85	88.60	91.28	91.01	88.97	78.08	62.45	14.53	38.42	42.94	13.54	29.95	40.46	16.61
Sm	13.74	11.68	25.22	9.54	13.07	18.15	18.2	7.51	16.99	17.02	17.36	16.08	14.80	13.84	3.82	10.73	8.66	3.98	6.19	8.18	3.69
Eu	2.79	0.91	3.92	1.83	2.53	3.18	2.53	2.17	2.76	3.36	3.15	2.73	2.80	2.41	0.97	2.62	2.25	1.67	1.58	2.42	0.76
Gd	12.99	9.82	22.29	8.68	12.04	16.99	16.72	5.99	15.17	15.27	15.68	13.53	13.09	13.35	6.53	9.87	7.65	4.09	5.93	7.70	3.97
Tb	2.17	1.85	3.69	1.28	1.93	2.78	2.66	0.76	2.68	2.53	2.66	2.25	2.29	2.40	1.13	1.37	1.28	0.68	0.98	1.34	0.64
Dy	13.36	13.33	23.05	7.1	12.38	17.53	16.51	3.82	15.84	15.23	16.91	14.27	14.88	15.76	7.18	9.29	8.55	4.54	6.49	8.29	4.51
Ho	2.94	2.51	4.93	1.44	2.54	3.74	3.5	0.83	3.36	3.27	3.39	3.13	3.24	3.43	1.56	1.65	1.82	0.99	1.39	1.72	1.02
Er	8.6	7.87	13.43	3.81	7.43	10.4	9.71	2.18	9.73	9.38	10.16	8.34	9.08	9.45	6.26	5.11	5.16	2.59	3.54	4.85	2.71
Tm	1.23	1	1.97	0.54	1.09	1.5	1.46	0.33	1.40	1.37	1.47	1.23	1.27	1.36	0.35	0.93	0.78	0.36	0.54	0.71	0.44
Yb	9.32	6.16	14.72	4.07	8.2	10.94	10.27	2.48	9.87	9.74	10.62	8.83	9.43	9.83	1.54	5.36	6.24	2.76	4.08	4.94	2.87
Lu	1.26	0.82	2.09	0.62	1.13	1.52	1.47	0.4	1.38	1.45	1.53	1.35	1.29	1.42	0.81	0.77	0.84	0.35	0.52	0.70	0.42
Hf	15.03	8.01	31.25	11.33	15.2	19.6	16.98	9.28	18.96	22.17	19.54	18.61	16.24	24.35	3.82	6.55	7.04	2.48	4.69	6.86	3.30
Ta	4.2	2.63	5.55	2.59	4.65	4.1	5.1	5.94	3.23	3.97	5.13	3.12	3.49	3.43	1.55	2.08	2.28	1.15	1.52	1.39	0.85
Th	29.36	49.89	48.54	21.84	30.92	27.96	34.49	48.47	22.37	18.76	25.49	19.85	17.36	27.43	2.08	6.29	3.11	0.88	4.73	8.49	3.20
U	6.33	4.03	1.95	0.4	5.03	2.03	3.53	7.23	2.19	1.82	3.15	0.72	1.94	3.12	b.d.	0.24	0.41	b.d.	2.1	1.19	1.81
∑REE	430.21	373.42	767.86	335.08	504.62	609.44	672.78	389.24	563.61	524.18	542.73	546.95	469.81	481.38	100.89	274.31	238.1124	80.41734	175.5943	231.13	112.32

b.d Below detection limit